



Electrochemical Characterization of Low-Cost Lithium-Iron Orthosilicate Samples as Cathode Materials of Lithium-Ion Battery

M. M. Kalantarian^{a*}, M. Oghbaei^b, S. Asgari^b, L. Karimi^c, S. Ferrari^d, D. Capsoni^d, M. Bini^d, P. Mustarelli^d

^aDepartment of Ceramic, Materials and Energy research Center, Karaj, Iran.

^bDepartment of Materials Science and Engineering, Sharif University of Technology, Tehran, Iran.

^cFaculty of Chemistry, Department of Public Science, K. N. Toosi University of Technology, Tehran, Iran.

^dDepartment of Chemistry, Section of Physical Chemistry, University of Pavia, Pavia, Italy.

PAPER INFO

Paper history:

Received 31 July 2017

Accepted in revised form 12 December 2017

Keywords:

Electrochemistry

Lithium-ion Battery

Cathode

Lithium Iron Orthosilicate

Synthesis

Characterization

ABSTRACT

Lithium-iron-orthosilicate is one of the most promising cathode materials for Li-ion batteries due to its safety, environmental brightness and potentially low cost. In order to produce a low cost cathode material, $\text{Li}_2\text{FeSiO}_4/\text{C}$ samples are synthesized via sol-gel (SG; one sample) and solid state (SS; two samples with different carbon content) methods, starting from Fe(III) as the raw materials (low pristine materials). The three samples are characterized for purity, structure, and morphology. The electrochemical tests showed the different charge-discharge behaviors of the SS and SG samples. Electrochemical behaviors were investigated in terms of voltage vs. square root of capacity diagrams and their slopes. The best results are obtained for the SS sample containing the larger amount of carbon.

1. INTRODUCTION

Ever-growing demand of portable electronic devices calls for the development of more powerful rechargeable solid-state batteries. In this field, lithium-ion batteries outperform other systems due to their design flexibility and high energy density [1,2]. Moreover, global environmental concerns, as well as recent fluctuations in crude-oil prices, do lead to enhanced efforts for growth of lithium batteries for large-scale applications such as plug-in hybrid electric vehicles (P-HEVs) [3]. To date, cost and safety are critical issues that barred the use of lithium batteries in large scale applications [1]. Typically, oxide cathode materials were proposed for their appreciable performances and stability, but some safety problems, such as the risk of explosive accident caused by oxygen extraction in charge condition at elevated temperature, were also reported [4,5]. This problem could be solved by using strong covalent bonds to fix all the oxygen atoms in the poly-anion framework [4,6], this paved the way to the use of structurally stable iron based poly-

anion materials instead of lithium cobalt oxides, thus solving also the cost problem by using Fe instead of Co as transition metal [4]. An alternative poly-anion cathode material is lithium iron-orthosilicate ($\text{Li}_2\text{FeSiO}_4$) [7-12]. This material is interesting in view of price, thermal stability [13], environmental friendship and, finally, the possibility to extract up to two Li ions per formula unit [7]. Most interesting, iron and silicon are among the most abundant elements in nature and are environmentally benign, thus reducing costs and improving safety [8,11,13]. The most used synthesis routes reported in literature to prepare $\text{Li}_2\text{FeSiO}_4$ are based on the use of expensive Fe^{2+} sources as the pristine materials [9,10,12,14-19]; this fact and the problem of stabilizing the +2 oxidation state in the $\text{Li}_2\text{FeSiO}_4$ sacrifices the privilege of the low cost.

In this study $\text{Li}_2\text{FeSiO}_4$ was synthesized as a low cost cathode material for lithium batteries by using Fe^{+3} in the pristine materials. The samples were prepared following two different routes: sol-gel (SG) and solid state reaction (SS) methods. Generally, sol-gel is more expensive synthesis route than solid-state [20,21]. Carbon sources have been used to reduce iron from +3 to +2 oxidation state, as well as to guarantee the electric conduction during operation. Sol-gel synthesis route using iron(III) nitrate was performed to synthesis

*Corresponding Author's Email: m.kalantarian@merc.ac.ir (M. M. Kalantarian)

$\text{Li}_2\text{FeSiO}_4$ by many researchers [22-30]. A noble solid-state reaction (SS) method is the other synthesis method used in this work. Using low cost Fe_2O_3 pristine material makes the SS method a very simple and low cost synthesis route. Although our simple SS method is novel, a number of works had used Fe_2O_3 as pristine material (solid-state [31], hydrothermal [32] and sol-gel [33]). The observed different voltage-capacity behaviour in charge-discharge measurements for SG and SS samples is discussed on the basis of a lithium (de)intercalation mechanism [34].

2. EXPERIMENTAL

$\text{Li}_2\text{FeSiO}_4/\text{C}$ nano-composites were synthesized by sol-gel and solid-state reaction methods. In the sol-gel synthesis route, lithium acetate (Merck), iron(III) nitrate (Merck) and tetra-ethyl orthosilicate (TEOS, Aldrich) were used as pristine materials. Ethylene glycol (Merck) and citric acid (Merck) were added to TEOS in the 1 : $\frac{1}{3}$: 1 molar ratio. After 1 h mixing via magnetic stirring, lithium acetate and then iron(III) nitrate were added to the solution, which was kept at rest overnight in order to obtain the sol. Then, it was dried at 80 °C for 24 h, then ground and calcined in a horizontal silica tube furnace under Argon atmosphere at 700 °C for 1 h with a heating rate of 6 °C/min.

Solid-state reaction synthesis was performed via lithium silicate (Li_2SiO_3 , CHEMOS), iron(III) oxide (Fe_2O_3 , Aldrich) and glucose ($\text{C}_6\text{H}_{12}\text{O}_6$, Aldrich) as the carbon source for both carbon coating and reduction of iron(III) to iron(II). Two samples with different amounts of glucose, i.e. 19 and 38 wt.%, were prepared. The corresponding carbon amount in the pristine material was 8 and 16 wt.% (samples named SS-8C and SS-16C, respectively). The precursor materials were ground in an agate mortar and calcined at 700 °C for 7 h. The heating rate was 6 and 3 °C/min for SS-8C and SS-16C samples, respectively.

XRPD measurements were performed in air on a Bruker D5005 diffractometer with the $\text{Cu-K}\alpha$ radiation, graphite monochromator and scintillation detector. The patterns have been collected in the 2θ range of 15-66°. Rietveld structural and profile refinement was carried out by means of TOPAS V3.0 program [35].

Scanning Electron Microscopy (SEM) micrographs were obtained at 20 kV using a Hitachi S4160 microscope.

The electrochemical tests were performed using a three-electrodes T-cell with stainless steel current collectors, lithium metal as the negative electrode and a glasswool (Whatman GF/A) disc as the separator. The electrolyte was 1M LiPF_6 in ethylene carbonate/diethyl carbonate (EC/DEC) 1:1 (Merck). In order to prepare the cathode layer, a slurry was made by mixing the active material with carbon black (Alfa) and poly[vinylidene fluoride]

(PVdF, Solvay) in N-methyl-2-pyrrolidone solvent (NMP, Aldrich) with weight ratio of 80:10:10. The obtained suspensions were spread on an aluminum foil and dried at 80 °C overnight. The cell was assembled in a glove-box under argon atmosphere (MBraun, <1ppm O_2 , <1ppm H_2O). The galvanostatic cycling tests were carried out at different current rates using an Arbin battery cycler (model BT2000), between 2 and 4.63 V at room temperature.

3. RESULT AND DISCUSSION

The XRD patterns (Fig. 1) of the SG, SS-C8 and SS-C16 samples show the formation of the $\text{Li}_2\text{FeSiO}_4$, but also the presence of some impurity phases depended on both the synthesis route and the carbon amount.

To completely address the polymorphic phase of $\text{Li}_2\text{FeSiO}_4$ among the possible ones ($\text{P}2_1$ and $\text{P}2_1/n$ monoclinic; $\text{P}mn2_1$ and $\text{P}mnb$ orthorhombic structures) and the impurity phases amount, a Rietveld refinement was carried out on the collected patterns. The structural refinement confirms the formation of the monoclinic $\text{P}2_1/n$ polymorph in all samples, in agreement with the literature for samples treated in this temperature range [19,36]. Table 1 reports the main refined parameters and identification and amount of the impurity phases. A higher degree of purity is obtained in the SG sample, which also shows the smaller crystallites size, as obtained by the Scherrer relationship. Concerning the SS samples, the main impurity phases are the FeO and Li_2SiO_3 ; Fe metal is present in small amounts only in the SS-C16 sample, due to the use of a large amount of carbon source acting as a reducing agent. Fig. 1 shows the experimental and calculated patterns obtained by the Rietveld refinement.

TABLE 1. Lattice parameters, crystallites size and weight percentage of the $\text{Li}_2\text{FeSiO}_4$ phase in the samples. Impurity phase weight percentage and refinement discrepancy factor are also reported

		SG	SS-C8	SS-C16
$\text{Li}_2\text{FeSiO}_4$	$a / \text{\AA}$	8.2189	8.2530(28)	8.2373(19)
	$b / \text{\AA}$	5.0013	5.0206(13)	5.0158(7)
	$c / \text{\AA}$	8.247	8.2297(30)	8.2226(20)
	$\beta / \text{\AA}$	98.814	99.063(16)	99.087(16)
	Crystallite size /nm	26.1	67.6	55.4
	Weight percentage	98.62	92.69	91.81
Impurity phases	Halite	1.38	--	--
	magnetite	--	0.86	0.16
	FeO	--	3.5	1.2
	Li_2SiO_3	--	2.95	5.97
	Fe	--	--	0.86
Goodness of Fit	1.55	1.11	1.07	

The samples prepared by solid-state reaction were indeed less pure. This was likely due to the relatively low temperature of synthesis. However, heating at 900

°C would lead to an unwanted relevant increase of the average particle size.

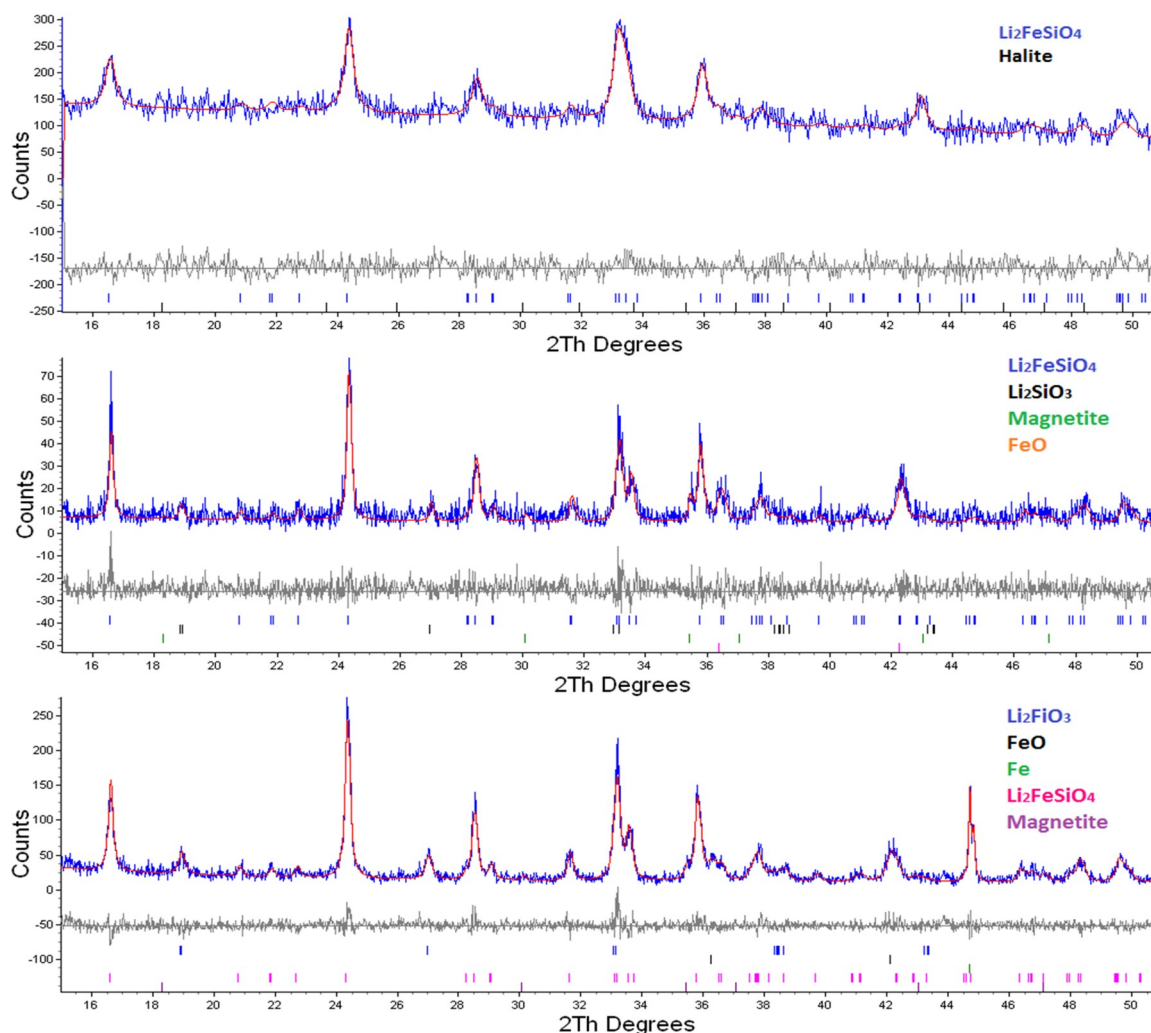


Figure 1. Rietveld refinement plots of the SG, SS-C8 and SS-C16 samples. Comparison of the experimental (blue) and calculated (red) patterns. The difference curve (gray) and the peaks positions for the different phases used in the refinement (bars) are also shown

Fig. 2 shows the SEM micrographs of the samples. The observed morphology is almost similar among the three samples, and consists of nano-sized grains that aggregate in larger particles, whose dimension is dependent of the synthesis procedure. The grains sizes determined by SEM (30, 70 and 55 nm for SG, SS-C8 and SS-C16, respectively) are in fairly good agreement with those extracted by XRD peaks broadening (see Table 1). Generally, as far as C/20 of applied current rate would be considered, the lower grain size resulted in the better performance. For the other C-rates (C/16 and C/10), there would be the other operating mechanism (as it will be discussed).

Fig. 3 shows the discharge capacity of the samples for current rates of C/20 (40 cycles), C/16 (10 cycles) and

C/10 (10 cycles). Charge capacity of each cycle was a little bit more than the discharge one (as it is usually observed), so, it is not reported here. In the first cycles of the SG and the SS-16C samples, the extraction of more than one electron per formula unit was obtained at C/20 current rate. The initial capacity of the SG, SS-8C and SS-16C samples were 195, 133 and 186 mAh.g⁻¹, respectively, corresponding to the extraction of 1.17, 0.80 and 1.12 electrons per formula unit. The discharge capacity fades after 30 cycles at C/20 rate to 91, 50 and 90% of the theoretical capacity for the SG, SS-8C and SS-16C samples, respectively. At all investigated current rates (C/20, C/16 and C/10), the worst discharge capacity and capacity retention were obtained for the SS-C8 sample. The obtained results of SG and SS-16C are comparable with previously published works [9,10,

24, 26, 37-41]. Although, high performance $\text{Li}_2\text{FeSiO}_4$ cathodes were reported in literature [22, 27, 29, 32, 37, 42-44], new approach to evaluate the $\text{Li}_2\text{FeSiO}_4$ electrochemical characterization (Figs. 4 and 5) is completely noble in this paper.

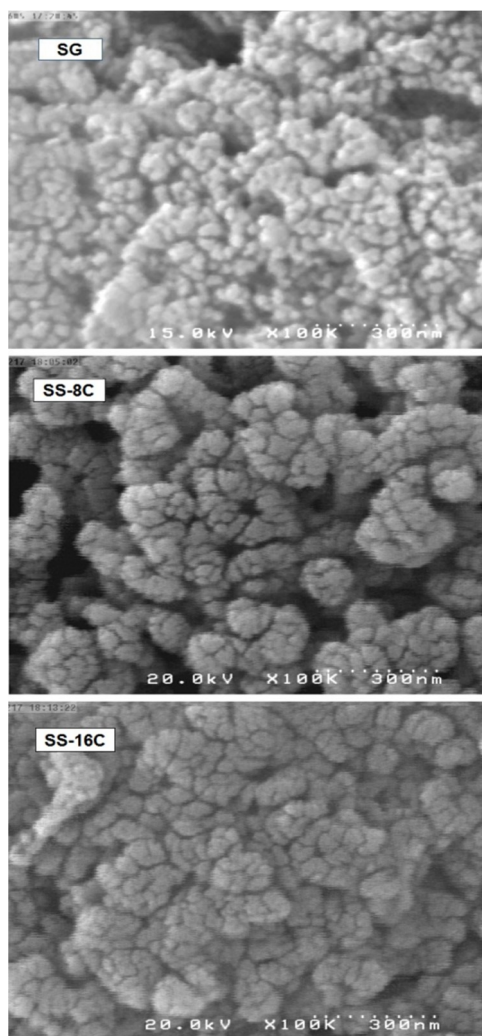


Figure 2. Scanning electron microscopy (SEM) images of the investigated samples

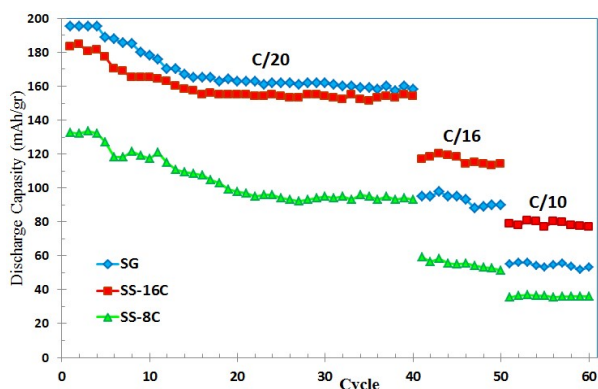


Figure 3. Obtained discharge capacity (mA.h.g^{-1}) of the samples for different applied current rates (mA.g^{-1})

Evaluation of synthesis methods is one of the aims of this paper, therefore, post-synthesis modification treatments were not performed for the powders. Obviously, modification treatments of the synthesized powders (for example ball-milling [42]) may improve performance of the cells, however, the results of this paper obtained from as-received powders are comparable with the results obtained from modified powders [22,27,29,32,37,42-44].

As far as concerns the SG and SS-16C samples, similar discharge capacity values were observed at C/20, but for higher current rates the SS-16C sample shows better electrochemical performances. According to our recent findings [45], this fact may be explained by the presence of a larger amount of impurities in the SS-16C sample, which, in turn, could lead to a higher rate capability. It was observed that impurities could increase rate capability of cathodes [46-49]. We have suggested that rate capability of such a cathode material is related to inversely-biased-diode phenomenon [49]. Impurities would cause remarkable enhancement of electronic conductivity by failing the inversely-biased-diode effect [49].

As far as concerns the SG and SS-16C samples, similar discharge capacity values were observed at C/20, but for higher current rates the SS-16C sample shows better electrochemical performances. According to our recent findings [45], this fact may be explained by the presence of a larger amount of impurities in the SS-16C sample, which, in turn, could lead to a higher rate capability. It was observed that impurities could increase rate capability of cathodes [46-49]. We have suggested that rate capability of such a cathode material is related to inversely-biased-diode phenomenon [49]. Impurities would cause remarkable enhancement of electronic conductivity by failing the inversely-biased-diode effect [49].

Fig. 4 shows the charge-discharge cycles for the samples. A different behaviour can be observed for the solid-state samples and the sol-gel one. In the case of the SS samples, in fact, the slope of the plateau is nearly constant during cycling, whereas the SG sample shows a slope increase with cycling. Based on our recent findings [34], plotting voltage versus the square root of capacity ($V - \sqrt{C}$) for charge-discharge measurements could give useful information about Li (de)intercalation mechanisms, as well as about microstructural (irreversible) changes. In particular, for $\text{Li}_2\text{FeSiO}_4$, it is demonstrated that voltage deviations are caused by formation of non-stoichiometric delithiated phases ($\text{Li}_{1.5}\text{FeSiO}_4$ and $\text{Li}_{0.5}\text{FeSiO}_4$) during charge/discharge, due to Li concentration gradients.

The linear dependence between voltage and the square root of capacity is given by Eq. 1. The lines slope of $V - \sqrt{C}$ diagrams is related to reaction energy (E_r), and

the square roots of lithium diffusion coefficient (D^*) and average particle diameter (d):

$$V = V_0 + a_3 E_r \sqrt{D^*} \sqrt{d} \sqrt{C} \quad (1)$$

Following our previous analysis [34], the main linear portion of the graphs reported in Fig. 4 could be attributed to the reaction (2).

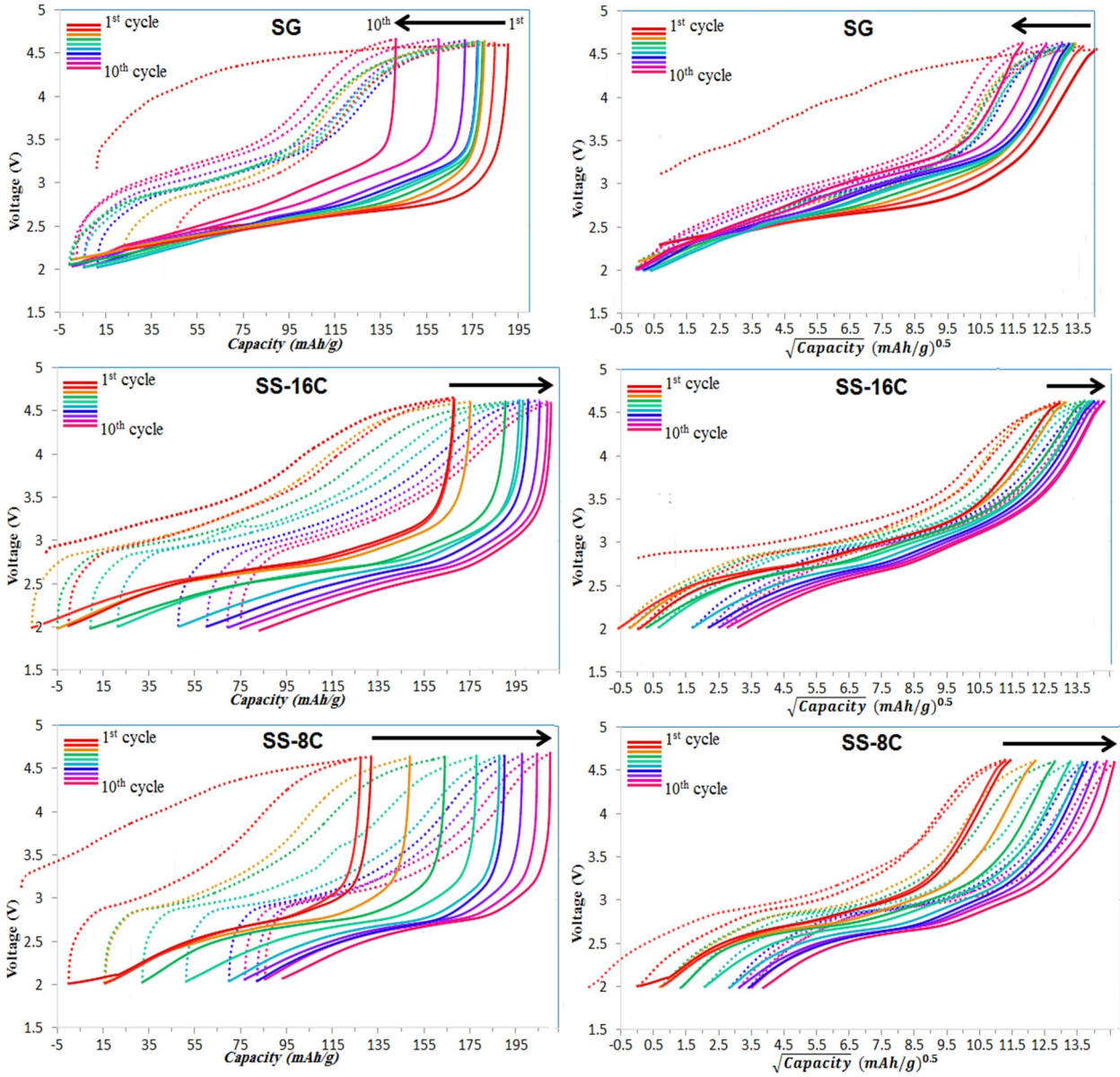
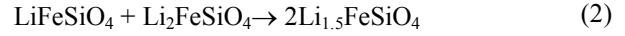


Figure 4. Voltage vs. capacity (left column) and voltage vs. square root of capacity (right column) obtained from charge-discharge measurements of the three samples. The diagrams are plotted for the first 10 cycles at $C/20$. Charge/Discharge curves are shown by dash/solid lines. The scale of the horizontal axes is attributed to the 2nd charge cycle and it is given only for the sake of comparison (hence, some curves fall outside the graphs)

Fig. 5 shows the behaviour of the slopes of the $V - \sqrt{C}$ diagrams (discharge curves) of Fig. 4 for the first 20 cycles. It should be noted that the voltage slope $V - \sqrt{C}$ of SG sample does increase by increasing the cycle number, whereas this quantity is almost constant for the solid-state samples. The marked variation ($\sim 170\%$)

observed for the SG sample is the indication of a lower reversibility of charge/discharge reaction in this sample with respect to the SS ones, where the variation is less than 20%. This can be attributed to the increase of the average particles size and/or to the decrease of the lithium diffusion coefficient, e.g. because of a

progressive material amorphization, as it was previously reported in the literature [50].

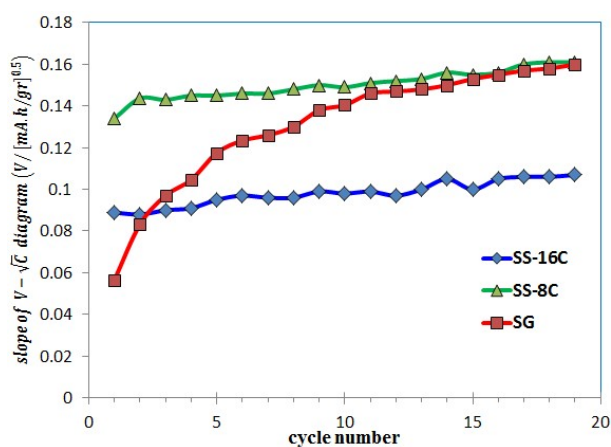


Figure 5. Behavior of the slopes of the $V - \sqrt{C}$ diagrams (discharge curves) of the samples for the first 20 cycles. The plateau of each diagram of Fig. 4 was considered to estimate the slope

4. CONCLUSIONS

Three samples of $\text{Li}_2\text{FeSiO}_4$ were synthesized and characterized as cathode materials for Li-ion batteries. They were prepared by using Fe^{+3} as the iron source in the pristine materials, and they have $\text{P}2_1/n$ monoclinic structure. Quite pure $\text{Li}_2\text{FeSiO}_4$ (99 %wt) was obtained by the sol-gel route, starting from iron (III) nitrate. Concerning the electrochemical properties, in C/20 of rate, obtained capacity of SS-16C and SG samples were in the same range, but fading of capacity under cycling for SG sample was more than that of the SS-16C. Considering the cyclability, according to $V - \sqrt{C}$ diagrams, the SS samples showed better reversibility of the charge/discharge reaction compared with the SG one. At rates higher than C/20, the best performances were offered by SS-16C. Regarding the rate-capability, the higher capacity was obtained in the higher rates for SS-16C sample in comparison with SG. Bypassing the rate-capability mechanisms called *inversely-biased-diode phenomena* is suggested to justify the better rate capability of SS-16C.

5. ACKNOWLEDGMENTS

The corresponding author acknowledge research grant (No.:271255) by Materials and Energy Research Center (MERC), Karaj, Iran.

REFERENCES

1. Tarascon, J.-M. and Armand, M., "Issues and challenges facing rechargeable lithium batteries", *Nature*, Vol. 414, (2001), 359-367.
2. Fisher, C.A., Kuganathan, N. and Islam, M.S., "Defect chemistry and lithium-ion migration in polymorphs of the cathode material $\text{Li}_2\text{MnSiO}_4$ ", *Journal of Materials Chemistry*, Vol. 1, (2013), 4207-4214.
3. Sun, Y.-K., Myung, S.-T., Park, B.-C., Prakash, J., Belharouak, I. and Amine, K., "High-energy cathode material for long-life and safe lithium batteries", *Nature Materials*, Vol. 8, (2009), 320-324.
4. Nishimura, S.-i., Kobayashi, G., Ohoyama, K., Kanno, R., Yashima, M. and Yamada, A., "Experimental visualization of lithium diffusion in Li_xFePO_4 ", *Nature Materials*, Vol. 7, (2008), 707-711.
5. Kazazi, M., Iilbeigi, M., Fazlali, A. and Mohammadi, A.H., "Preparation, characterization and stability of Li-ion conducting $\text{Li}_{1.5}\text{Al}_{0.5}\text{Ge}_{1.5}(\text{PO}_4)_3$ glass-ceramic with NASICON-type structure", *Journal of Advanced Ceramics Progress*, Vol. 2, (2016), 38-43.
6. Gong, Z. and Yang, Y., "Recent advances in the research of polyanion-type cathode materials for Li-ion batteries", *Energy & Environmental Science*, Vol. 4, (2011), 3223-3242.
7. Xu, B., Qian, D., Wang, Z. and Meng, Y.S., "Recent progress in cathode materials research for advanced lithium ion batteries", *Materials Science and Engineering: R: Reports*, Vol. 73, (2012), 51-65.
8. Kalantarian, M.M., Asgari, S., Capsoni, D. and Mustarelli, P., "An ab initio investigation of $\text{Li}_2\text{M}_{0.5}\text{N}_{0.5}\text{SiO}_4$ (M, N = Mn, Fe, Co Ni) as Li-ion battery cathode materials", *Physical Chemistry Chemical Physics*, Vol. 15, (2013), 8035-8041.
9. Nytén, A., Abouimrane, A., Armand, M., Gustafsson, T. and Thomas, J. O., "Electrochemical performance of $\text{Li}_{2-x}\text{FeSiO}_4$ as a new Li-battery cathode material", *Electrochemistry Communications*, Vol. 7, (2005), 156-160.
10. Nytén, A., Kamali, S., Häggström, L., Gustafsson, T. and Thomas, J.O., "The lithium extraction/insertion mechanism in $\text{Li}_2\text{FeSiO}_4$ ", *Journal of Materials Chemistry*, Vol. 16, (2006), 2266-2272.
11. Armstrong, A.R., Kuganathan, N., Islam, M.S. and Bruce, P.G., "Structure and lithium transport pathways in $\text{Li}_2\text{FeSiO}_4$ cathodes for lithium batteries", *Journal of the American Chemical Society*, Vol. 133, (2011), 13031-13035.
12. Sirisopanaporn, C., Masquelier, C., Bruce, P.G., Armstrong, A. R. and Dominko, R., "Dependence of $\text{Li}_2\text{FeSiO}_4$ Electrochemistry on Structure", *Journal of the American Chemical Society*, Vol. 133, (2010), 1263-1265.
13. Dominko, R., Arçon, I., Kodre, A., Hanžel, D. and Gaberšček, M., "In-situ XAS study on $\text{Li}_{2-x}\text{MnSiO}_4$ and $\text{Li}_{2-x}\text{FeSiO}_4$ cathode materials", *Journal of Power Sources*, Vol. 189, (2009), 51-58.
14. Zaghbi, K., Ait Salah, A., Ravet, N., Mauger, A., Gendron, F. and Julien, C., "Structural, magnetic and electrochemical properties of lithium iron orthosilicate", *Journal of Power Sources*, Vol. 160, (2006), 1381-1386.
15. Sirisopanaporn, C., Boulineau, A., Hanzel, D., Dominko, R., Budic, B., Armstrong, A.R., Bruce, P.G. and Masquelier, C., "Crystal structure of a new polymorph of $\text{Li}_2\text{FeSiO}_4$ ", *Inorganic Chemistry*, Vol. 49, (2010), 7446-7451.
16. Gao, K., Zhang, J. and Li, S.-D., "Morphology and electrical properties of $\text{Li}_{2-x}\text{FeSiO}_4$ prepared by a vacuum solid-state reaction", *Materials Chemistry and Physics*, (2013).
17. Huang, X., Li, X., Wang, H., Pan, Z., Qu, M. and Yu, Z., "Synthesis and electrochemical performance of $\text{Li}_{2-x}\text{FeSiO}_4$ /carbon/carbon nano-tubes for lithium ion battery", *Electrochimica Acta*, Vol. 55, (2010), 7362-7366.
18. Boulineau, A., Sirisopanaporn, C., Dominko, R., Armstrong, A.R., Bruce, P.G. and Masquelier, C., "Polymorphism and

- structural defects in $\text{Li}_2\text{FeSiO}_4$ ", *Dalton Transactions*, Vol. 39, (2010), 6310-6316.
19. Bini, M., Ferrari, S., Ferrara, C., Mozzati, M.C., Capsoni, D., Pell, A.J., Pintacuda, G., Canton, P. and Mustarelli, P., "Polymorphism and magnetic properties of Li_2MSiO_4 (M= Fe, Mn) cathode materials", *Scientific Reports*, Vol. 3, (2013).
 20. Asadi Tabrizi, R., Hesarakhi, S. and Zamanian, A., " Effects of time, temperature and precursor on solid state synthesis of α -TCP", *Journal of Advanced Ceramics Progress*, Vol. 1, (2015), 36-39.
 21. Esfandiari, S., Honarvar Nazari, H., Nemati, A., Kargar Razi, M. and Baghshahi, S., "Characterization of Structural, Optical and Hydrophilicity properties of TiO_2 Nano-Powder Synthesized by Sol-Gel Method", *Journal of Advanced Ceramics Progress*, Vol. 2, (2016), 1-6.
 2. Fisher, C.A., Kuganathan, N. and Islam, M.S., "Defect chemistry and lithium-ion migration in polymorphs of the cathode material $\text{Li}_2\text{MnSiO}_4$ ", *Journal of Materials Chemistry*, Vol. 1, (2013), 4207-4214.
 3. Sun, Y.-K., Myung, S.-T., Park, B.-C., Prakash, J., Belharouak, I. and Amine, K., "High-energy cathode material for long-life and safe lithium batteries", *Nature Materials*, Vol. 8, (2009), 320-324.
 4. Nishimura, S.-i., Kobayashi, G., Ohoyama, K., Kanno, R., Yashima, M. and Yamada, A., "Experimental visualization of lithium diffusion in Li_xFePO_4 ", *Nature Materials*, Vol. 7, (2008), 707-711.
 5. Kazazi, M., Iilbeigi, M., Fazlali, A. and Mohammadi, A.H., "Preparation, characterization and stability of Li-ion conducting $\text{Li}_{1.5}\text{Al}_{0.5}\text{Ge}_{1.5}(\text{PO}_4)_3$ glass-ceramic with NASICON-type structure", *Journal of Advanced Ceramics Progress*, Vol. 2, (2016), 38-43.
 6. Gong, Z. and Yang, Y., "Recent advances in the research of polyanion-type cathode materials for Li-ion batteries", *Energy & Environmental Science*, Vol. 4, (2011), 3223-3242.
 7. Xu, B., Qian, D., Wang, Z. and Meng, Y.S., "Recent progress in cathode materials research for advanced lithium ion batteries", *Materials Science and Engineering: R: Reports*, Vol. 73, (2012), 51-65.
 8. Kalantarian, M.M., Asgari, S., Capsoni, D. and Mustarelli, P., "An ab initio investigation of $\text{Li}_2\text{M}_{0.5}\text{N}_{0.5}\text{SiO}_4$ (M, N= Mn, Fe, Co Ni) as Li-ion battery cathode materials", *Physical Chemistry Chemical Physics*, Vol. 15, (2013), 8035-8041.
 9. Nyttén, A., Abouimrane, A., Armand, M., Gustafsson, T. and Thomas, J. O., "Electrochemical performance of $\text{Li}_2\text{FeSiO}_4$ as a new Li-battery cathode material", *Electrochemistry Communications*, Vol. 7, (2005), 156-160.
 10. Nyttén, A., Kamali, S., Häggström, L., Gustafsson, T. and Thomas, J.O., "The lithium extraction/insertion mechanism in $\text{Li}_2\text{FeSiO}_4$ ", *Journal of Materials Chemistry*, Vol. 16, (2006), 2266-2272.
 11. Armstrong, A.R., Kuganathan, N., Islam, M.S. and Bruce, P.G., "Structure and lithium transport pathways in $\text{Li}_2\text{FeSiO}_4$ cathodes for lithium batteries", *Journal of the American Chemical Society*, Vol. 133, (2011), 13031-13035.
 12. Sirisopanaporn, C., Masquelier, C., Bruce, P.G., Armstrong, A. R. and Dominko, R., "Dependence of $\text{Li}_2\text{FeSiO}_4$ Electrochemistry on Structure", *Journal of the American Chemical Society*, Vol. 133, (2010), 1263-1265.
 13. Dominko, R., Arčon, I., Kodre, A., Hanžel, D. and Gaberšček, M., "In-situ XAS study on $\text{Li}_2\text{MnSiO}_4$ and $\text{Li}_2\text{FeSiO}_4$ cathode materials", *Journal of Power Sources*, Vol. 189, (2009), 51-58.
 14. Zaghbi, K., Ait Salah, A., Ravet, N., Mauger, A., Gendron, F. and Julien, C., "Structural, magnetic and electrochemical properties of lithium iron orthosilicate", *Journal of Power Sources*, Vol. 160, (2006), 1381-1386.
 15. Sirisopanaporn, C., Boulineau, A., Hanzel, D., Dominko, R., Budic, B., Armstrong, A.R., Bruce, P.G. and Masquelier, C., "Crystal structure of a new polymorph of $\text{Li}_2\text{FeSiO}_4$ ", *Inorganic Chemistry*, Vol. 49, (2010), 7446-7451.
 16. Gao, K., Zhang, J. and Li, S.-D., "Morphology and electrical properties of $\text{Li}_2\text{FeSiO}_4/\text{C}$ prepared by a vacuum solid-state reaction", *Materials Chemistry and Physics*, (2013).
 17. Huang, X., Li, X., Wang, H., Pan, Z., Qu, M. and Yu, Z., "Synthesis and electrochemical performance of $\text{Li}_2\text{FeSiO}_4/\text{carbon}/\text{carbon nano-tubes}$ for lithium ion battery", *Electrochimica Acta*, Vol. 55, (2010), 7362-7366.
 18. Boulineau, A., Sirisopanaporn, C., Dominko, R., Armstrong, A.R., Bruce, P.G. and Masquelier, C., "Polymorphism and structural defects in $\text{Li}_2\text{FeSiO}_4$ ", *Dalton Transactions*, Vol. 39, (2010), 6310-6316.
 19. Bini, M., Ferrari, S., Ferrara, C., Mozzati, M.C., Capsoni, D., Pell, A.J., Pintacuda, G., Canton, P. and Mustarelli, P., "Polymorphism and magnetic properties of Li_2MSiO_4 (M= Fe, Mn) cathode materials", *Scientific Reports*, Vol. 3, (2013).
 20. Asadi Tabrizi, R., Hesarakhi, S. and Zamanian, A., " Effects of time, temperature and precursor on solid state synthesis of α -TCP", *Journal of Advanced Ceramics Progress*, Vol. 1, (2015), 36-39.